crystals

MDPI

Communication

Numerical Analysis of the Combined Influence of Accelerated Crucible Rotation and Dynamic Crucible Translation on Liquid Phase Diffusion Growth of SiGe

Mandeep Sekhon [1,*], Brian Lent [1] and Yanbao Ma [2]

[1] Crystal Growth Laboratory, University of Victoria, Victoria, BC V8W3P6, Canada; blent@uvic.ca
[2] Water and Energy Laboratory, University of California at Merced, Merced, CA 95343, USA; yma5@ucmerced.edu
* Correspondence: mssekhon@uvic.ca; Tel.: +1-209-7359599

Academic Editor: Bing Gao
Received: 25 July 2016; Accepted: 6 September 2016; Published: 13 September 2016

Abstract: The effects of accelerated crucible rotation technique (ACRT) and dynamic translation on liquid phase diffusion (LPD) growth of Si_xGe_{1-x} single crystals have been separately investigated numerically in earlier works and were found to have a very positive impact on the LPD growth process. Building upon these findings, in this paper, we study the consequences of imposing both ACRT and dynamic translation on this growth technique. Time-dependent, axisymmetric numerical simulations using moving grid approach have been carried out using finite volume code Ansys Fluent. Crucible translation effect is simulated using dynamic thermal boundary condition. Results are compared to the case in which this growth system is subjected to ACRT only. It is predicted that by combining ACRT with dynamic pulling, excellent axial compositional uniformity can be achieved and growth rate can be improved substantially without significantly compromising on the benefits of employing ACRT. The results show that it is advantageous to utilize the combination of ACRT and dynamic translation during LPD growth rather than using them independently for producing relatively uniform composition Si_xGe_{1-x} single crystals in a shorter span of time.

Keywords: liquid phase diffusion; simulation; germanium-silicon alloys; accelerated crucible rotation technique; dynamic translation; modeling; solution growth; numerical study

1. Introduction

Si_xGe_{1-x} is an upcoming alloy semiconductor material that is gaining prominence because its properties can be adjusted as per the needs of a particular application [1]. This is due to the fact that this alloy system displays a complete solid and liquid state miscibility. On the downside, this system also exhibits a wide gap between the solidus and liquidus lines making it difficult to grow uniform composition Si_xGe_{1-x} crystals using the well-known melt growth techniques [2]. Some of the applications of this material include photodetectors, high-performance discrete devices, heterodevices, solar cells, and substrate for epitaxial growth [1,3].

Liquid phase diffusion (LPD) is a solution growth technique that has been used to grow axially graded composition single crystals of Si_xGe_{1-x} [4]. The complete details of the LPD growth process can be found in [4].

In order to produce an axially uniform composition crystal, the growth interface should be maintained at a constant temperature. To accomplish this, the crucible should be pulled downwards at a rate equal to the growth rate. The effect of crucible translation with the objective of growing uniform Si_xGe_{1-x} crystals has been investigated in the literature [5–7]. In the work [7], an automatic

feedback control system was developed with dynamic pull correction after every minute and resulted in a 23 mm long crystal with uniform composition.

The effect of constant and dynamic pull rate on the LPD growth was studied in [8]. Numerical simulation results showed that by translating the crucible in a dynamic fashion the interface temperature could be maintained at a nearly constant value and consequently uniform axial crystal composition could be achieved. Furthermore, the results also indicated that the growth time could be reduced considerably by employing dynamic translation.

In the accelerated crucible rotation technique (ACRT) developed in [9], the crucible undergoes acceleration and deceleration cyclically and is used to generate flow in the melt/solution crystal growth techniques. In the spin up and spin down period of the ACRT, Ekman layer flow is produced at the solid surface creating a radial flow and fluid also experiences spiral shearing [10]. A large body of work exists in the literature studying the effects of ACRT experimentally and numerically on the melt and solution growth techniques (see for instance [11–21]), and it has been found in many studies that the application of ACRT leads to an improvement in the melt mixing, growth rate, radial compositional uniformity, and solid/liquid interface flattening.

In the numerical work [22] on the LPD growth process, it was found that the growth interface was concave in shape for a large fraction of the simulated growth period. To achieve uniformity in the radial crystal composition along the growth interface, the shape of the interface should be flat. In a recent work on this growth system [23], the effect of imposing ACRT on the LPD growth was examined numerically. It was predicted that by utilizing the ACRT cycle at 12 rpm, the growth interface could be made nearly flat which in turn helped in substantially improving the uniformity in radial composition along the growth interface.

Motivated by the positive effects of dynamic translation and ACRT on the LPD growth, in this work, we have investigated the impact of the combination of ACRT and dynamic pulling numerically. The simulation results reveal that by superimposing dynamic translation on ACRT, the uniform axial composition can be achieved with a significant improvement in the growth rate while retaining the key advantages of using ACRT.

2. Numerical Simulation

From a numerical point of view, LPD comes under the category of the moving boundary problem. In order to draw a valid comparison with the earlier work [23], we have followed the same dynamic grid approach to handle the moving boundary. The simulations have been carried out using the finite volume based software Ansys Fluent (ANSYS, Inc., Canonsburg, PA, USA) by developing special user defined functions to move the mesh nodes. Triangular ACRT cycle (at 12 rpm) was used to carry out the computation.

It is important to highlight that the governing equations in the case of a moving grid approach involve additional terms to account for the grid motion. The grid flux in the discretized equations must be computed from space conservation law or else there is a possibility of the creation of artificial mass sources [24]. In Ansys Fluent, the problem of the artificial mass source is avoided as the space conservation law is used while computing grid flux [25]. The position of the initial growth interface was determined based on the isotherm corresponding to the melting point of germanium. The mesh is comprised of 4674, 1518, 656, 1002 quadrilateral elements in the melt, seed, source, and quartz regions, respectively. Further refining of the mesh did not result in any significant change in the solution. Pressure-velocity coupling was dealt with using the PISO algorithm [26] and a time step size of 0.1 s was adopted. A smaller time step did not change the solution while a larger time step resulted in convergence problems. The absolute convergence criterion [27] was used to judge convergence and the solution was considered converged when residuals had fallen below 10^{-4} for continuity, radial and axial momentum equations and below 10^{-6} for concentration and energy equations. The domain of the problem is comprised of silicon source at the top, the Si-Ge melt in the middle, the Ge-seed below, and the vertical wall of the quartz ampoule (see Figure 1). It must be noted that some of the results

presented in this paper were obtained by writing special user defined functions in Ansys Fluent as they were not directly available from the GUI of Ansys Fluent.

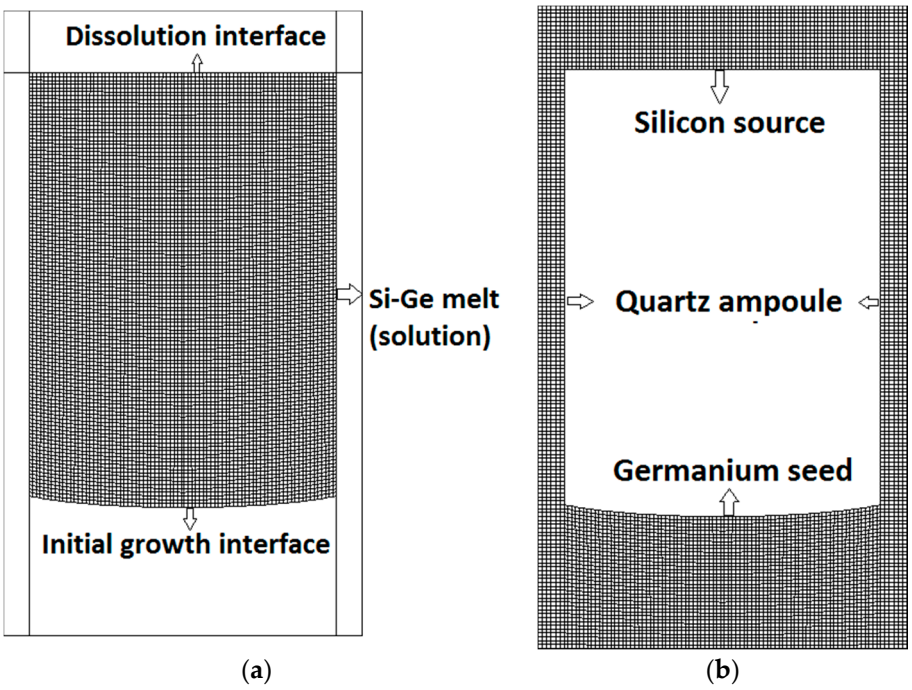

Figure 1. Initial computational mesh used for numerical simulation in the (**a**) Liquid subdomain (**b**) Solid subdomains.

The governing equations are the Continuity, Momentum Balance, Energy Balance and Mass Transport equations. The complete set of governing equations can found in the previous paper [23] and are not repeated here. It is assumed that the same temperature gradient exists below the initial position of the crucible based on the experimental observations. A complete list of assumptions can be found in earlier work [28]. As mentioned before, to simulate the effects of crucible translation dynamic thermal boundary conditions were prescribed and the details can be found in the work [8]. For the boundary and initial conditions for the concentration and velocity fields, the reader is referred to the paper [23]. The details regarding the implementation of the dynamic grid approach in Ansys Fluent for the LPD growth process can be found elsewhere [28].

3. Results and Discussions

While carrying out the numerical simulations, the crucible subjected to accelerated crucible rotation (triangular cycle at 12 rpm) was pulled dynamically after 5 h of growth time. The pull rate was adjusted after completion of one or more ACRT cycles in order to maintain a nearly uniform crystal composition along the centerline. A comparison is made with the previously examined case in which only ACRT is applied to the ampoule [23].

It is important to note that after early hours of growth, LPD becomes a diffusion dominated process [22] and consequently in the later hours of growth the flow is mainly generated due to the application of ACRT [23]. The ACRT induced flow structure does not alter much with the addition of dynamic translation and it can be observed from Figure 2 that there is a minor drop in the maximum radial velocity near the growth interface with the incorporation of dynamic pulling.

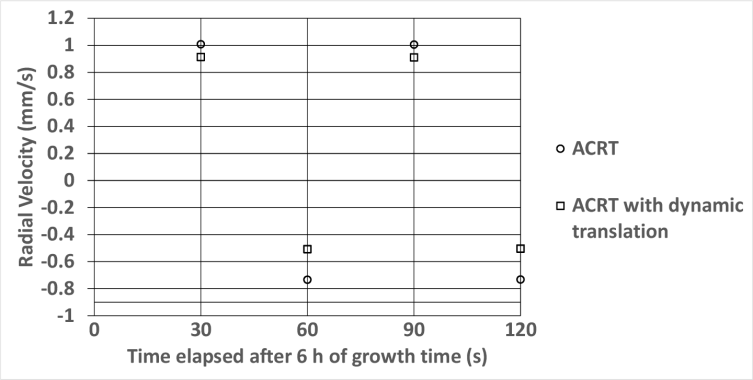

Figure 2. Maximum outward and inward radial velocities in the vicinity of the growth interface after 6 h of growth time.

As shown in Figure 3, the concentration difference along the growth interface increases slightly as dynamic pulling is superimposed on ACRT. This can be attributed to the increase in the temperature difference along the growth interface in the case of combined ACRT and dynamic pulling (see Figure 4). It can be readily observed from Figure 5 that the interface temperature at the centerline becomes nearly constant with the application of dynamic translation. This, in turn, leads to a nearly constant centerline crystal composition in the axial direction as shown in Figure 6.

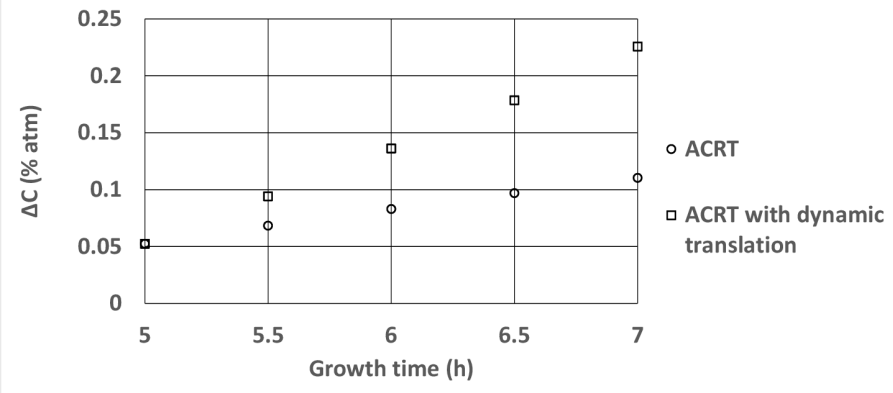

Figure 3. Difference between crystal composition at the wall and at the centerline along the growth interface.

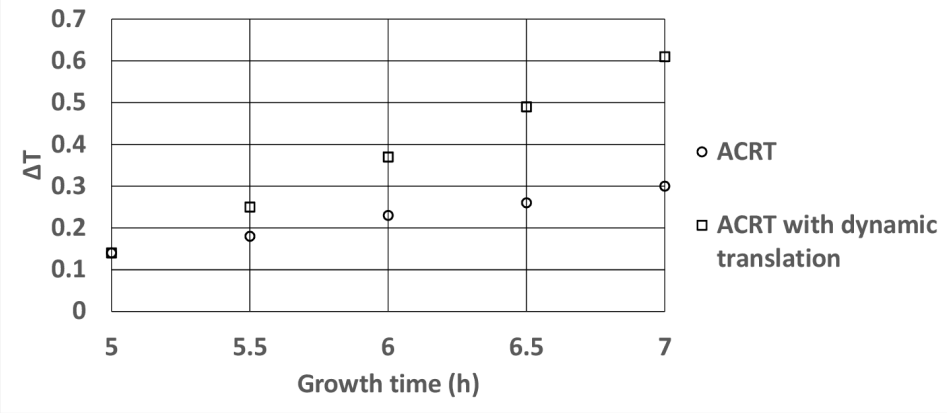

Figure 4. Difference between temperature at the wall and at the centerline along the growth interface.

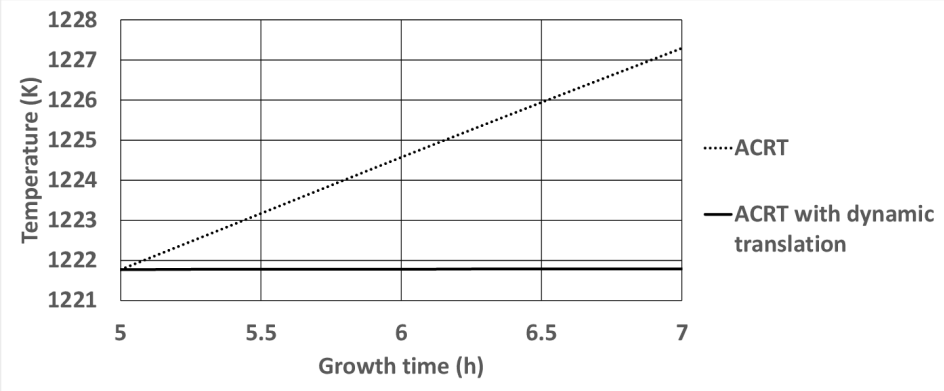

Figure 5. Variation of the interface temperature at the centerline with growth time after the initiation of dynamic translation (t = 5 h).

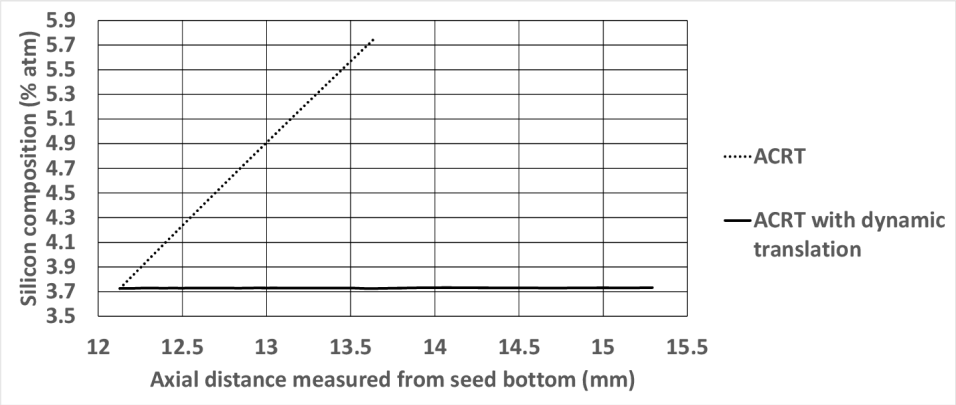

Figure 6. Variation of the axial crystal composition at the centerline after the initiation of dynamic translation (t = 5 h).

A dramatic increase in both instantaneous and time averaged growth velocity with the inclusion of dynamic translation can be clearly seen in Figure 7 and Table 1, respectively. This explains the greater interface displacement after 7 h of growth time observed in Figure 8 when using the combination of ACRT and dynamic pulling instead of ACRT alone. Moreover, it can also be inferred from Figure 8 that dynamic pulling does not have any significant detrimental impact on the interface flattening effect of ACRT.

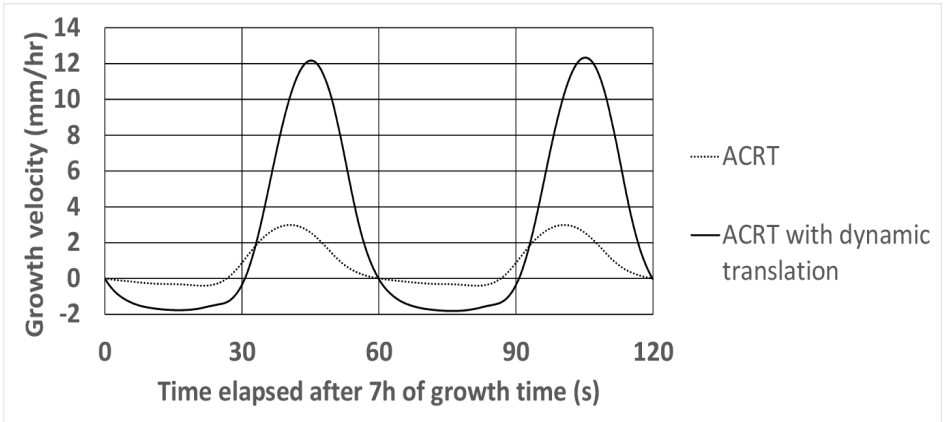

Figure 7. Growth velocity variation at the centerline during a single ACRT cycle at t = 7 h.

Table 1. Variation of the time averaged growth velocity at the centerline with growth time after the initiation of dynamic translation (t = 5 h).

Growth Time (h)	Growth Velocity (mm/h) at the Centerline (ACRT) (Data from [23])	Growth Velocity (mm/h) at the Centerline (ACRT with Dynamic Translation)
5.5	0.760	1.328
6	0.763	1.613
6.5	0.760	2.025
7	0.755	2.599

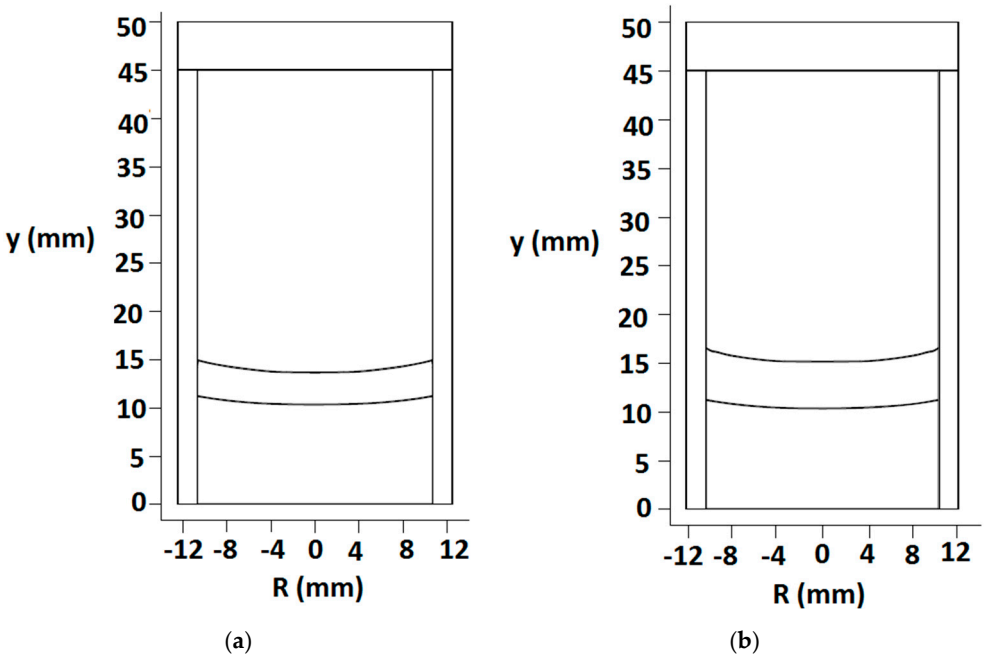

Figure 8. Interface displacement in 7 h of growth time (**a**) ACRT, (**b**) ACRT with dynamic translation.

The dynamic pull profile shown in Figure 9 was obtained by running the simulation in an intermittent manner. After the completion of each ACRT cycle (120 s), the simulation was stopped and the crystal composition along the growth interface at the centerline was checked. The pull rate was adjusted if the crystal composition value was found to be changing significantly. The simulation process was then continued with this new pull rate value for another cycle. The whole process was then repeated to obtain a nearly constant crystal composition along the growth interface at the centerline. The pull rate values and the corresponding time intervals for which it was maintained, were recorded throughout the simulation process and are depicted in Figure 9. It should be noted that due to numerical difficulties related to mesh quality the simulations could not be accurately carried out further. Nevertheless, the simulation results clearly bring out the potential benefits of using the combination of ACRT and dynamic translation for the LPD growth system.

It can be observed from Figure 9 that the dynamic pull profile shows an upward trend and is about to reach its maximum value. This can be explained on the basis of the underlying physics of the LPD growth process. LPD is a solution growth technique and works on the principle of saturation and precipitation. The difference in the liquidus equilibrium composition (solubility limit) and the actual concentration near the growth interface is the driving force for this growth process. The liquidus equilibrium composition near the growth interface is a function of the melt temperature. During the early hours of growth, the melt temperature is relatively high and hence the liquidus equilibrium composition is also high. Moreover, the actual amount of silicon dissolved in the melt near the growth interface is quite small. Hence, the driving potential for growth is high and results in the increase

of the growth velocity. As mentioned earlier, in order to grow axially uniform composition crystal, pull rate should match the growth velocity. Consequently, an upward trend in the dynamic pull profile is observed in Figure 9. As the growth process continues, dynamic pulling should result in an appreciable reduction of the melt temperature and hence the liquidus equilibrium composition near the growth interface should also decrease. Also, with the passage of time, the actual silicon concentration in the melt near the growth interface increases significantly. As a result, the overall driving potential for the growth process should reduce and lead to the reduction of the growth velocity. Thus, it can be expected that dynamic pull rate should start decreasing after reaching its peak value.

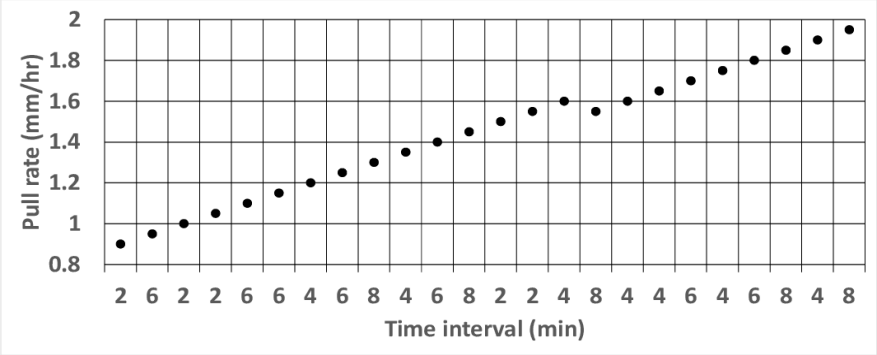

Figure 9. Dynamic pull profile between t = 5 h and t = 7 h.

4. Conclusions

This paper builds upon the earlier works on the LPD growth process in which the effects of ACRT and dynamic translation were examined separately [8,23]. A comparison is drawn to the case when the crucible is only subjected to ACRT. It is found that the combination of ACRT and dynamic translation does not alter the flow structure significantly. The concentration difference along the growth interface is found to increase slightly with the inclusion of dynamic translation. It is predicted that temperature and hence crystal composition at the centerline of the growth interface becomes nearly constant with the usage of dynamic pulling. Furthermore, this combination leads to a significant improvement in instantaneous and time averaged growth velocity without deteriorating the interface flattening effect of ACRT. This study shows promising results of the combined effects of ACRT and dynamic translation on the LPD growth. The combined ACRT and dynamic translation processes need further optimization to find the best LPD growth process, which requires a more systematic experimental study.

Author Contributions: Mandeep Sekhon carried out the simulations and drafted the paper. Brian Lent conceived the idea and significantly contributed to the correction and improvement of the manuscript. Yanbao Ma helped in the interpretation of results, critically reviewed the paper, and made important suggestions for its improvement.

Conflicts of Interest: The authors declare no conflict of interest.

References

1. Kasper, E. Prospects of SiGe heterodevices. *J. Cryst. Growth* **1995**, *150*, 921–925. [CrossRef]
2. Abrosimov, N.V.; Rossolenko, S.N.; Thieme, W.; Gerhardt, A.; Schröder, W. Czochralski growth of Si- and Ge-rich SiGe single crystals. *J. Cryst. Growth* **1997**, *174*, 182–186. [CrossRef]
3. Deitch, R.H.; Jones, S.H.; Diggers, T.G., Jr. Bulk single crystal growth of silicon-germanium. *J. Electron. Mater.* **2000**, *29*, 1074–1078. [CrossRef]
4. Yildiz, M.; Dost, S.; Lent, B. Growth of bulk SiGe single crystals by liquid phase diffusion. *J. Cryst. Growth* **2005**, *280*, 151–160. [CrossRef]
5. Nakajima, K.; Kodama, S.; Miyashita, S.; Sazaki, G.; Hiyamizu, S. Growth of Ge-rich Si_xGe_{1-x} single crystal with uniform composition (x = 0.02) on a compositionally graded crystal for use as GaAs solar cells. *J. Cryst. Growth* **1999**, *205*, 270–276. [CrossRef]

6. Azuma, Y.; Usami, N.; Ujihara, T.; Sazaki, G.; Murakami, Y.; Miyashita, S.; Fujiwara, K.; Nakajima, K. Growth of SiGe bulk crystal with uniform composition by directly controlling the growth temperature at the crystal–melt interface using in situ monitoring system. *J. Cryst. Growth* **2001**, *224*, 204–211. [CrossRef]
7. Azuma, Y.; Usami, N.; Ujihara, T.; Fujiwara, K.; Sazaki, G.; Murakami, Y.; Nakajima, K. Growth of SiGe bulk crystals with uniform composition by utilizing feedback control system of the crystal–melt interface position for precise control of the growth temperature. *J. Cryst. Growth* **2003**, *250*, 298–304. [CrossRef]
8. Sekhon, M.; Armour, N.; Dost, S. Numerical and experimental investigation of the effect of crucible translation in liquid phase diffusion growth of SiGe. *J. Cryst. Growth* **2015**, *412*, 7–15. [CrossRef]
9. Scheel, H.J.; Schulz-Dubois, E.O. Flux growth of large crystals by accelerated crucible-rotation technique. *J. Cryst. Growth* **1971**, *8*, 304–306. [CrossRef]
10. Schulz-Dubois, E.O. Accelerated crucible rotation: Hydrodynamics and stirring effect. *J. Cryst. Growth* **1972**, *12*, 81–87. [CrossRef]
11. Capper, P.; Gosney, J.J.G.; Jones, C.L. Application of the accelerated crucible rotation technique to the Bridgman growth of $Cd_xHg_{1-x}Te$: Simulations and crystal growth. *J. Cryst. Growth* **1984**, *70*, 356–364. [CrossRef]
12. Coates, W.G.; Capper, P.; Jones, C.L.; Gosney, J.J.G.; Ard, C.K.; Kenworthy, I.; Clark, A. Effect of ACRT rotation parameters on Bridgman grown $Cd_xHg_{1-x}Te$ crystals. *J. Cryst. Growth* **1989**, *94*, 959–966. [CrossRef]
13. Xu, Y.-B.; Fan, S.-J. Accelerated crucible rotation technique: Bridgman growth of $Li_2B_4O_7$ single crystal and simulation of the flows in the crucible. *J. Cryst. Growth* **1993**, *133*, 95–100. [CrossRef]
14. Moon, S.J.; Kim, C.-J.; Ro, S.T. Effects of buoyancy and periodic rotation on the melt flow in a vertical Bridgman configuration. *Int. J. Heat Mass Transf.* **1997**, *40*, 2105–2113. [CrossRef]
15. Lan, C.W.; Chian, J.H. Effects of ampoule rotation on vertical zone-melting crystal growth: Steady rotation versus accelerated crucible rotation technique (ACRT). *J. Cryst. Growth* **1999**, *203*, 286–296. [CrossRef]
16. Yeckel, A.; Derby, J.J. Effect of accelerated crucible rotation on melt composition in high-pressure vertical Bridgman growth of cadmium zinc telluride. *J. Cryst. Growth* **2000**, *209*, 734–750. [CrossRef]
17. Okano, Y.; Kondo, H.; Dost, S. Numerical study of interface shape control in the VGF growth of compound semiconductor crystal. *J. Cryst. Growth* **2002**, *237–239*, 1769–1772. [CrossRef]
18. Bloedner, R.U.; Gille, P. Growth of $Hg_{1-x}Cd_xTe$ single crystals by travelling heater method under accelerated crucible rotation conditions. *J. Cryst. Growth* **1993**, *130*, 181–187. [CrossRef]
19. Brunskill, I.H.; Boutellier, R.; Depmeier, W.; Schmid, H.; Scheel, H.J. High-temperature solution growth of $Pb(Fe_{0.5}Nb_{0.5})O_3$ and $Pb(Mn_{0.5}Nb_{0.5})O_3$ crystals. *J. Cryst. Growth* **1982**, *56*, 541–546. [CrossRef]
20. Masalov, V.M.; Emel'chenko, G.A.; Mikhajlov, A.B. Hydrodynamics and oscillation of temperature in single crystal growth from high-temperature solutions with use of ACRT. *J. Cryst. Growth* **1992**, *119*, 297–302. [CrossRef]
21. Barz, R.U.; Sabhapathy, P.; Salcudean, M. A numerical study of convection during THM growth of CdTe with ACRT. *J. Cryst. Growth* **1997**, *180*, 566–577. [CrossRef]
22. Yildiz, M.; Dost, S. A continuum Model for the Liquid Phase Diffusion Growth of Bulk SiGe Single Crystals. *Int. J. Eng. Sci.* **2005**, *43*, 1059–1080. [CrossRef]
23. Sekhon, M.; Lent, B.; Dost, S. Numerical study of liquid phase diffusion growth of SiGe subjected to accelerated crucible rotation. *J. Cryst. Growth* **2016**, *438*, 90–98. [CrossRef]
24. Demirdžić, I.; Perić, M. Space conservation law in finite volume calculations of fluid flow. *Int. J. Numer. Methods Fluids* **1988**, *8*, 1037–1050. [CrossRef]
25. ANSYS Inc. *Ansys Fluent 14.5 Theory Guide 2012*; ANSYS Inc.: Canonsburg, PA, USA, 2012.
26. Issa, R.I. Solution of the implicitly discretised fluid flow equations by operator-splitting. *J. Comput. Phys.* **1986**, *62*, 40–65. [CrossRef]
27. ANSYS Inc. *Ansys Fluent 14.5 User's Guide 2012*; ANSYS Inc.: Canonsburg, PA, USA, 2012.
28. Sekhon, M.; Dost, S. Numerical examination of the effect of steady crucible rotation in the liquid phase diffusion growth of SiGe. *J. Cryst. Growth* **2015**, *430*, 63–70. [CrossRef]